Potential Energy Landscape for Hot Electrons in Periodically Nanostructured Graphene

B. Borca,[1] S. Barja,[1,2] M. Garnica,[1,2] D. Sánchez-Portal,[3,4,*] V. M. Silkin,[3,4,5] E. V. Chulkov,[3,4,6] C. F. Hermanns,[1]
J. J. Hinarejos,[1,7] A. L. Vázquez de Parga,[1,2,7,†] A. Arnau,[3,4,6] P. M. Echenique,[3,4,6] and R. Miranda[1,2,7]

[1]*Departamento de Física de la Materia Condensada, Universidad Autónoma de Madrid, Cantoblanco, 28049 Madrid, Spain*
[2]*Instituto Madrileño de Estudios Avanzados en Nanociencia (IMDEA Nanociencia), Cantoblanco, 28049 Madrid, Spain*
[3]*Centro de Física de Materiales (CSIC-UPV/EHU), Materials Physics Center (MPC),*
Paseo Manuel de Larzidaval 5, 20018 San Sebastian, Spain
[4]*Donostia International Physics Centre (DIPC), Paseo de Manuel Lardizabal 4, 20018 San Sebastian, Spain*
[5]*IKERBASQUE, Basque Foundation for Science, 48011 Bilbao, Spain*
[6]*Departamento de Física de Materiales (UPV/EHU), Facultad de Química, Apartado 1072, 20080 San Sebastian, Spain*
[7]*Instituto "Nicolás Cabrera", Universidad Autónoma de Madrid, Cantoblanco 28049, Madrid, Spain*

We explore the spatial variations of the unoccupied electronic states of graphene epitaxially grown on Ru(0001) and observed three unexpected features: the first graphene image state is split in energy; unlike all other image states, the split state does not follow the local work function modulation, and a new interfacial state at $+3$ eV appears on some areas of the surface. First-principles calculations explain the observations and permit us to conclude that the system behaves as a self-organized periodic array of quantum dots.

PACS numbers: 73.20.−r, 68.37.Ef, 68.55.−a, 73.22.Pr

Lateral superlattices in graphene, a form of carbon with unique electronic properties [1], can be realized by periodic arrays of doping centers, electronic and geometric corrugations [2] or externally applied potentials [3]. They have been predicted to show a number of intriguing properties such as anisotropic propagation of charge carriers [3], miniband transport and even new quasiparticles for triangular superlattices [4]. A lateral superlattice consisting of regions of graphene with different electronic properties can easily be prepared by thermal decomposition of hydrocarbons on metallic substrates [5,6]. This process results in an epitaxial graphene monolayer with a periodic array of bumps and valleys (termed ripples) originating from the lattice mismatch between graphene and the different substrates, which provide us with a tunable pattern of structural and electronic heterogeneities [7].

The electronic structure of graphene can be modified by the substrate by doping with electrons or holes or by inducing a periodic modulation in the density of states or both effects simultaneously [2,8]. In particular, graphene grown on Ru(0001) is an ideal model system to study the interaction of graphene with a metallic substrate because the chemical interaction is spatially modulated with a periodicity of only 31.1 Å [9–11]. Close to the Fermi level, this spatially-periodic chemical interaction modulates the electronic structure producing an ordered array of electron pockets [2]. The unoccupied electronic states of these graphene superlattices, however, have not been characterized or discussed so far, in spite of their relevance for the dynamics of hot electrons. These states could also be important to understand the graphene intercalated compounds [12] where the so-called interlayer state, recently

identified as the first image state [13], plays a crucial role in the superconducting properties [14].

Particularly relevant among the unoccupied states are the image states, bound by the image-charge response of metallic surfaces and with a free-electron like dispersion parallel to the surface [15]. In scanning tunneling microscopy (STM) experiments the electric field across the tunnel junction causes a Stark shift of these states expanding the image state spectrum into a resonance spectrum. These field emission resonances (FERs) were experimentally observed in field ion microscopy by Jason [16] and with STM by Binnig *et al.* [17] and, since then, they have been used to identify different metals at surfaces [18] or to study modulations on the surface work function [19,20].

In this Letter, we explore by means of scanning tunneling microscopy and spectroscopy and first-principles calculations the periodic modulation of the unoccupied electronic states in graphene/Ru(0001), mapping the potential energy landscape for hot electrons in this lateral superlattice of graphene. Experimentally, we found three unexpected features in this system. The first graphene image state is localized on nanometer size regions where the distance between graphene and Ru(0001) is larger (H areas), while it is more extended on the L areas (smaller graphene Ru distance). This state does not shift in energy following the variation in work function from L to H areas. A new interfacial state at $+3$ eV appears in the L areas. First principles calculations explain the origin and characteristic of these spectral features.

The experiments were done in two ultra high vacuum chambers. One equipped with a variable temperature STM working between 80 K and 300 K, and the other with a low temperature STM working between 4.6 K and 77 K. The

tunneling spectra were measured with the feedback loop connected and the variation of the distance between tip and sample, Z, was recorded as a function of the bias voltage, V, applied. The $Z(V)$ curves were numerically differentiated to obtain the dZ/dV curves.

Figure 1(a) shows a STM image recorded on a Ru(0001) sample partially covered with graphene. The image shows the moiré superstructure that appears at this sample voltage as an ordered triangular array of bumps (right half of the image). The inset in Fig. 1(b) shows the dZ/dV curve measured on the clean Ru(0001) region. Three peaks reflecting the FERs are visible in the spectra. As usually expected, the first FER appears slightly above the work function of Ru(0001) [21]. Figure 1(b) shows the dZ/dV curves measured on the H and L areas of the moiré [blue (dark gray) and red (medium gray) curves, respectively]. In the curves measured on the H areas of the moiré, where the distance between graphene and the metal substrate is larger, the first FER appears around $+4.4$ eV, close to the average work function measured on this surface [21].

The curves measured on the L areas of the moiré, where the chemical interaction between graphene and ruthenium is stronger and, accordingly, the interlayer distance shorter, present some unexpected features. First, there is a new peak, 3 eV above the Fermi level, well below the vacuum level, which is not present in the H areas of the moiré. Second, the first FER (next peak in the curve) is located now at $+4.8$ eV, i.e., at higher energy than in the H areas. The energies of all higher order FERs are always smaller on the L areas than on the H areas, reflecting the difference in the local work function [22]. This is expected from theory and experiments in other systems [17]. The first FER at the L areas shows, however, an energy shift of about 0.4 eV with respect to the peak at H areas and in the opposite direction to the local work function change. This reversed shift of the f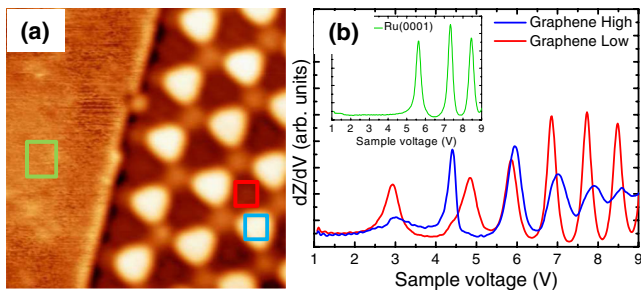irst FER is a robust result, which does not depend on the tip sharpness, sample temperature (in the range 4.6 K–300 K) or tunneling current used in the experiments, although the exact magnitude of the energy shift depends on the electric field between tip and sample [23].

Taking advantage of the spatial resolution of the STM, we map the spatial distribution of the spectral features discussed above. Figure 2(a) shows a 90×90 Å² STM topographical image of a single layer of graphene grown on Ru(0001) with the characteristic bright (H areas) and dark (L areas) regions and Figs. 2(b)–2(d) show the dZ/dV maps measured simultaneously at bias voltages corresponding, respectively, to the peak at $+3.0$ V and the first FER measured on the H and L areas of the moiré at $+4.4$ and $+4.8$ V. The dZ/dV map of the new peak at $+3.0$ V presents intensity only on the L areas of the moiré and shows a small intensity modulation, probably due to the different stacking sequence in the L areas of the moiré [24]. The spatial distribution of the $+4.4$ eV peak [Fig. 2(c)] reveals that the state is localized on the H areas. On the contrary, the dZ/dV map at $+4.8$ eV [Fig. 2(d)] shows localization of the state on the L areas with a modulation in the amplitude similar to Fig. 2(b).

In order to understand the origin of the new peak at $+3$ eV and the anomalous energy shift of the first FER, as well as the above mentioned different spatial localization of the FERs, we have performed two different sets of first-principles calculations based on density functional theory (DFT). First we have used the SIESTA code [25] to make an explicit description of the electronic and atomic structure of the substrate in order to characterize the (different) C-Ru interactions in the L and H areas. This calculation permits
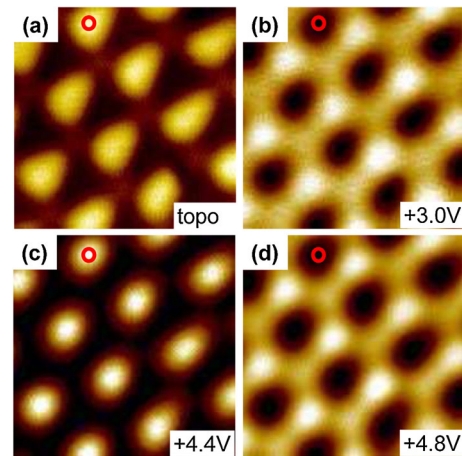

FIG. 1 (color online).   (a) STM image (150×150 Å², $V_s = -0.5$ V) measured at 4.6 K at the edge of a graphene island. The left-hand side is the uncovered Ru(0001) surface, while on the right-hand side the moiré superlattice of graphene appears as a triangular array of bumps. (b) dZ/dV curves measured on the moiré superstructure on the graphene island. The blue (dark gray) curve was measured in the H areas [blue (dark gray) box in (a)]. The red (medium gray) curve shows the corresponding spectra measured in the L areas of the moiré [red (medium gray) box in (a)]. Inset in (b) shows dZ/dV curve measured on the clean Ru(0001) [green (light gray) box in (a)].

FIG. 2 (color online).   (a) STM topographic image (90×90 Å², $V_s = -0.5$ V) measured simultaneously with the dZ/dV maps shown in the other panels. (b) dZ/dV map showing the spatial distribution of the new feature that appears at $+3$ V in the L areas of the moiré superstructure. (c) dZ/dV map showing the spatial distribution of the feature that appears in the spectra a $+4.4$ V. The intensity of this feature is strictly confined to the H areas of the moiré. (d) dZ/dV map showing that the feature that appears in the spectra a $+4.8$ V is confined to the L areas of the moiré. The red circle marks the same spot in all the images.
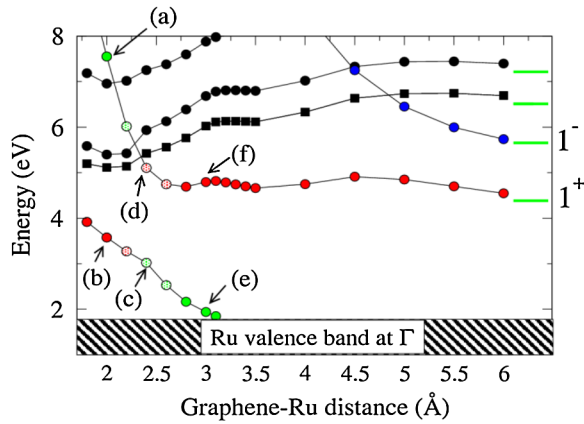
FIG. 3 (color online). The calculated evolution of the energies (relative to the Fermi level) of the unoccupied states at Γ, i.e., within the projected band gap of Ru(0001), when a laterally strained graphene layer is approached to the surface. The green horizontal lines, at the right-hand side, show the energy position of the states for a freestanding strained graphene layer with our basis set of numerical orbitals supplemented with diffuse orbitals. States labeled with 1^+ and 1^- correspond to the first and second image states [13]. The letters refer to the different panels of Fig. 4. Squares and circles indicate the doubly and singly degenerate states.

an unambiguous identification of the peak appearing at $+3$ eV on the L areas. The second set of calculations used plane waves and pseudopotentials to study the dependence of the field emission resonances on the applied electric field between tip and sample [26].

The actual structure of the graphene layer on Ru(0001) involves a very large (and complex) unit cell not yet fully understood [9,27]. This makes precise first-principles calculations on this system extremely demanding. For this reason, commensurate structures with graphene strained to match the Ru lattice parameter (2.7 Å) were used to identify the main dependence of the electronic structure on the graphene-Ru interlayer distance and registry [26]. Figure 3 shows the results obtained when a strained graphene plane with a top-hcp registry with respect to the Ru surface layer is moved towards the Ru(0001) surface. Very similar results are found for other stackings and here we just concentrate on the effect of the graphene-Ru distance. First, we will discuss the origin of the different bands. The green horizontal lines in Fig. 3 indicate the energy position of the states for a freestanding, but strained, graphene layer. The first two states correspond to the first two "image states" $(1^+, 1^-)$ described in Ref. [13]. These states are still bound to the layer using local or semilocal DFT, i.e., without the explicit inclusion of the image-potential tail. At large distances the main effect of the Ru substrate is to break the up-down symmetry of the layer, as well as to confine these extended states due to the gap that exists in the projected band structure at the relevant energy range. As a result, the 1^+ and 1^- states of graphene form linear combinations either with larger weight towards the

vacuum [red (medium gray) dots in Fig. 3] or in the interface region [blue (dark gray) dots]. The latter rapidly shift upwards in energy out of the window relevant for our experiments. On the contrary, the 1^+ state [red (medium gray) dots] stays constant in energy for graphene-Ru distances larger than 3.0 Å.

Approaching the graphene layer further we also induce the confinement of the electronic states of the Ru(0001) surface. In particular, a surface resonance of Ru [green (light gray) dots in Fig. 3] that is reminiscent of the surface states observed in the (111) surfaces of the noble metals and, for the clean Ru surface, appears slightly below the edge of the Ru(0001) projected band gap. When the distance between the graphene layer and the Ru(0001) surface is smaller than 3.0 Å, this resonance is promoted to a surface state and starts to hybridize with the first image state of graphene [points (e) and (f) in Fig. 3]. The corresponding charge distributions are shown in Figs. 4(e) and 4(f). For distances around 2.4 Å this resonance, strongly hybridized with graphene, appears near $+3$ eV [point (c) in Fig. 3]. Its corresponding charge distribution shows a remarkable increase in the charge above the graphene overlayer [Fig. 4(c)]. Simultaneously, the 1^+ image state strongly shifts upwards in energy, as seen in Fig. 3 [point (d)]. The corresponding charge distribution [Fig. 4(d)] clearly shows an increase in the charge density in the space between graphene and ruthenium. Below 2.4 Å an avoided crossing between the two bands can be seen in Fig. 3 [points (a),(b)] and Figs. 4(a) and 4(b).
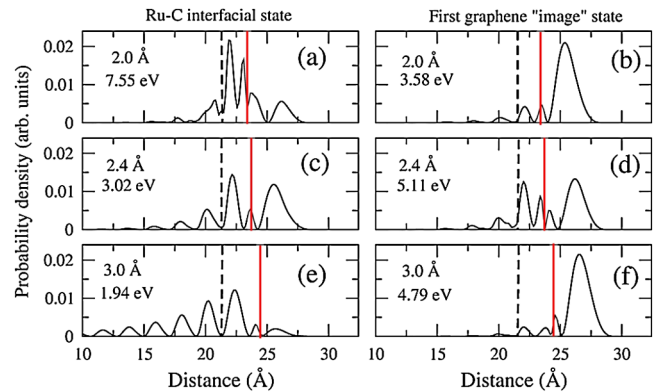

FIG. 4 (color online). Planar average of the density associated with selected states in our DFT calculations of strained graphene on Ru(0001). The dashed black line marks the Ru(0001) surface and the continuous red line the graphene plane. The letters of the panels correspond to the letters shown in Fig. 3. For a graphene-Ru distance $d = 3$ Å, relatively weak C-Ru interaction (H areas), the Ru surface resonance remains unchanged (e) while the first FER corresponds to the 1^+ image state modified by the neighboring Ru (f). At $d = 2.4$ Å (L areas), stronger interaction, the interfacial state displaces its charge appreciably outside the graphene layer due to the interlayer confinement (c), while the first FER has its charge distributed on both sides of the C surface (d). A further pushing of the C layer towards the metal to $d = 2$ Å reveals an avoided crossing of the two bands by the exchange in character of the states [(a) and (b)].

Experimentally we observed a resonance at $+3$ eV only in the L areas. We can now identify it with the rather broad Ru(0001) surface resonance lifted upwards (~ 1 eV) from the bottom of the projected band gap at Γ due to the C-Ru interaction. Similar dZ/dV spectra recorded on the moiré superstructure of graphene on Ir(111), where the graphene-Ir distance is larger, do not show a peak at $+3$ eV, supporting our identification as an interface peak related to the short C-Ru distance. The corresponding charge distribution is very sensitive to the graphene-Ru distance, as shown in Fig. 4. It corresponds to an interfacial state whose charge protrudes outside the graphene layer (allowing its detection by STM) only at short graphene-Ru distances.

The calculations also give an explanation for the reversed shift. As the graphene layer approaches the metal surface, the confinement and the hybridization with Ru states shift the 1^+ state upwards (by ~ 0.32 eV upon changing the C-Ru distance from 3.0 to 2.4 Å). In the L areas the local work function is smaller [22]; therefore, the 1^+ state is more extended towards the vacuum in the L areas and is more sensitive to the electric field applied between the STM tip and the surface [26]. This produces an additional upward shift of the first FER in L areas with respect to H areas. This relative shift amounts to ~ 0.5 eV for an electric field of 0.4 eV/Å [26]. The combined effect of the electric field and the Ru induced confinement overcompensates the change of the local work function from L to H areas and explains the reversed shift of the first FER.

What happens is that the effective potential felt by an electron in the 1^+ state is less repulsive in the H areas and can be pictured as a periodic array of shallow attractive (with respect to the average) potential wells of nanometer size associated with the H areas, i.e., forming a periodic array of quantum dots. This explains the strong localization of the peak at $+4.4$ eV in the H areas. In two dimensions any attractive potential of finite strength, under quite general conditions, has at least one bound state [28]. The situation for a periodic potential is slightly different [29], but the effect is similar: the splitting of the bottom of the free-electron-like 1^+ band into a quantum dotlike lower band ($+4.4$ eV) localized in the H areas and a higher band ($+4.8$ eV) more delocalized (dispersive) in the spatially connected L areas (see Fig. 2).

In conclusion, we have explored the potential energy landscape for hot electrons in a lateral superlattice of graphene grown on Ru(0001). Because of the spatial modulation of the interaction with the metallic substrate, the energy position of the first FER is not tied to the value of the local work function but splits into two subbands: the one at higher energy is localized over the extended L areas and the one at lower energy is localized at the H areas. The appearance of a new interfacial state was also discussed. Its energy position is strongly dependent on the graphene-Ru interaction and, thus, it can be used to calibrate the height of the graphene above the Ru surface. The spatial modulation of the first image state of graphene on Ru(0001) resembles that of a periodic array of quantum dots with low

binding energies. Interesting electron correlation effects can be expected when several electrons are simultaneously injected into this band.

*sqbsapod@sq.ehu.es
†al.vazquezdeparga@uam.es

[1] A. K. Geim and K. S. Novoselov, Nature Mater. **6**, 183 (2007).
[2] A. L. Vázquez de Parga et al., Phys. Rev. Lett. **100**, 056807 (2008).
[3] Ch.-H. Park et al., Nature Phys. **4**, 213 (2008).
[4] Ch.-H. Park et al., Phys. Rev. Lett. **101**, 126804 (2008).
[5] T. A. Land et al., Surf. Sci. **264**, 261 (1992).
[6] Ch. Oshima and A. Nagashima, J. Phys. Condens. Matter **9**, 1 (1997).
[7] A. B. Preobrajenski et al., Phys. Rev. B **78**, 073401 (2008).
[8] S. Y. Zhou et al., Nature Mater. **6**, 770 (2007).
[9] D. Martoccia et al., Phys. Rev. Lett. **101**, 126102 (2008).
[10] B. Wang et al., Chem. Phys. **10**, 3530 (2008).
[11] D. Jiang, M.-H. Du, and S. Dai, J. Chem. Phys. **130**, 074705 (2009).
[12] M. S. Dresselhaus and G. Dresselhaus, Adv. Phys. **51**, 1 (2002).
[13] V. M. Silkin et al., Phys. Rev. B **80**, 121408(R) (2009).
[14] G. Csányi et al., Nature Phys. **1**, 42 (2005).
[15] P. M. Echenique and J. B. Pendry, J. Phys. C **11**, 2065 (1978).
[16] A. J. Jason, Phys. Rev. **156**, 266 (1967).
[17] G. Binnig et al., Phys. Rev. Lett. **55**, 991 (1985).
[18] T. Jung, Y. W. Mo, and F. J. Himpsel, Phys. Rev. Lett. **74**, 1641 (1995).
[19] M. Pivetta et al., Phys. Rev. B **72**, 115404 (2005).
[20] P. Ruffieux et al., Phys. Rev. Lett. **102**, 086807 (2009).
[21] F. J. Himpsel et al., Surf. Sci. **115**, L159 (1982).
[22] T. Brugger et al., Phys. Rev. B **79**, 045407 (2009).
[23] See supplementary material at http://link.aps.org/supplemental/10.1103/PhysRevLett.105.036804 for experimental results showing the effect of the electric field between tip and sample on the energy position of the FERs.
[24] S. Marchini, S. Günther, and J. Wintterlin, Phys. Rev. B **76**, 075429 (2007).
[25] J. Soler et al., J. Phys. Condens. Matter **14**, 2745 (2002).
[26] See supplementary material at http://link.aps.org/supplemental/10.1103/PhysRevLett.105.036804 for details on the theoretical calculations and the results using plane waves.
[27] W. Moritz et al., Phys. Rev. Lett. **104**, 136102 (2010).
[28] B. Simon, Ann. Phys. (N.Y.) **97**, 279 (1976).
[29] B. Wunsch, F. Guinea, and F. Sols, New J. Phys. **10**, 103027 (2008).